

Generation of coherent radiation in the vacuum ultraviolet using randomly quasi-phase-matched strontium tetraborate

PETER TRABS,¹ FRANK NOACK,¹ ALEKSANDR S. ALEKSANDROVSKY,² ALEXANDRE I. ZAITSEV,² AND VALENTIN PETROV^{1,*}

¹Max-Born-Institute for Nonlinear Optics and Ultrafast Spectroscopy, 2A Max-Born-Str., D-12489 Berlin, Germany

²L. V. Kirensky Institute of Physics, Akademgorodok 50/38, Krasnoyarsk 660036, Russia

*Corresponding author: petrov@mbi-berlin.de

Received 3 November 2015; accepted 20 December 2015; posted 6 January 2016 (Doc. ID 253230); published 29 January 2016

Tunable coherent radiation is generated in the vacuum ultraviolet down to 121 nm using random quasi-phase matching in strontium tetraborate, the shortest wavelength ever produced with a second-order nonlinear optical process in a solid-state material. Relevant properties of this radiation, the nonlinear process, and the nonlinear crystal are investigated. © 2016 Optical Society of America

OCIS codes: (190.2620) Harmonic generation and mixing; (190.7110) Ultrafast nonlinear optics; (190.4400) Nonlinear optics, materials.

<http://dx.doi.org/10.1364/OL.41.000618>

Upconversion of coherent laser radiation to the vacuum ultraviolet (VUV) below 200 nm using second-order nonlinear optical processes in crystals is challenging mainly due to the lack of suitable materials that are simultaneously transparent, birefringent, and noncentrosymmetric. Nevertheless, the interest in such upconversion to this difficult spectral range for different applications is great because, in contrast to four-wave mixing (FWM) or harmonic generation in gases, such schemes can be easily implemented on any timescale (pulse duration and repetition rate) and, in particular, with unamplified (high repetition rate) ultrafast sources. Moreover, the reverse process of downconversion could be implemented for reliable temporal diagnostics of ultrashort pulses generated in the VUV by other methods.

From the crystals which offer birefringent phase matching below 200 nm, $\text{KBe}_2\text{BO}_3\text{F}_2$, or KBBF (under study for ~ 20 years, but still not commercially available), with point group 32, is definitely the most successful material: the shortest wavelength achieved by sum-frequency generation (SFG) in KBBF was 153.4 nm [1], although the average power amounted to only ~ 1 nW, since this wavelength is already very close to the 0-level cutoff wavelength of 147 nm [2]. Despite enormous difficulties related to its layered structure (growth, size, and cutting) KBBF remains a unique nonlinear crystal due to its relatively high nonlinear coefficient ($d_{11} = 0.47$ pm/V) and its large birefringence [2] which enables second-harmonic

generation (SHG) down to 161.1 nm, as well as phase matching for the fourth (by direct SHG) and fifth harmonic of Ti:sapphire laser systems [2]. Wavelengths below 150 nm, however, will be absorbed even by thin samples.

Reported attempts to fabricate quasi-phase matching (QPM) structures included mechanical twinning of crystalline quartz (SiO_2), with cutoff at 145 nm, which possesses trigonal 32 symmetry [3] and electric field poling of the ferroelectric MgBaF_4 (cutoff at 126 nm) which has mm2 symmetry [4]. Both materials exhibit much lower nonlinear coefficients compared to KBBF; the shortest wavelength experimentally reached so far by SHG with a fifth-order grating in quartz was 194 nm [3], while QPM has never been demonstrated in the UV with MgBaF_4 .

Random variation of the second-order susceptibility in acentric crystals leads to modification of the QPM conditions (random QPM or RQPM) and broadband spectral acceptance without pronounced dependence on the propagation direction [5]. It can be considered as an intermediate case between QPM and a non-phase-matched process where the generated power, though exhibiting irregular behavior, grows linearly with the propagation distance [5].

Random domains are known to form in ferroelectric materials, such as KTiOPO_4 (KTP), as a result of the phase transition in the cooling process during growth. Strontium tetraborate, SrB_4O_7 (SBO), which exhibits orthorhombic mm2 symmetry, the same as KTP or MgBaF_4 , is the first non-ferroelectric crystal for which spontaneous formation of such domains was encountered in the process of Czochralski growth [6]. The domains are in the form of sheets normal to the a -axis and rather homogeneous in the other two directions. The static polarization is parallel to the polar two-fold c -axis. Thus, the largest nonzero nonlinear coefficient that can be employed is d_{33} . The birefringence of SBO is too low (< 0.005) for phase matching. Non-phase-matched SHG has been realized in SBO for temporal diagnostics (autocorrelation measurements), but the efficiency of this process was extremely low when only one coherence length is utilized [7]. However, the bandgap wavelength (values from absorption measurements differ but indicate, in the best case, < 120 nm [7–9]), the good

damage resistivity, and chemical stability, as well as the exceptionally high ($1.5\text{--}3.5\text{ pm/V}$ [7,10]) value of the diagonal d_{33} element (with respect to the bandgap value), are features that make SBO very attractive for RQPM. Recently, this technique has been demonstrated to be very useful for frequency doubling of femtosecond pulses in the UV, such as generation of the fourth harmonic of a mode-locked 82 MHz Ti:sapphire oscillator in the 187.5–215 nm range [11]. Here we study the potential of RQPM SBO for frequency doubling of amplified femtosecond pulses at shorter wavelengths, covering the 121 to 172 nm spectral range with the second harmonic (SH).

Figure 1 shows the RQPM SBO sample available for the present experiment. After removal of the initial and final part along the a -axis where no domains were seen, the thickness of the sample became $\sim 0.88\text{ mm}$. The transversal dimensions were $6.4 \times 5.6\text{ mm}^2$ ($b \times c$). For comparison, a single domain SBO crystal with the same a -cut was used whose thickness amounted to 0.425 mm . Note that under the $c < a < b$ convention for the lattice constants [8] the correspondence with the dielectric frame is $abc \equiv yxz$ ($n_x < n_y < n_z$), which we confirmed by refractive index measurements in the visible with a prism, resolving a discrepancy in the literature [9].

While this RQPM SBO sample (S7) showed relatively large variation of the SH intensity across the aperture (Fig. 1, right), in the bottom left corner it yielded higher efficiency and less structured spectra compared to other samples [12]. We measured the transmission of the samples for $E//c$ at $\sim 160\text{ nm}$ (fifth harmonic of a Ti:sapphire regenerative amplifier at 1 kHz). The transmission of the RQPM SBO sample, measured with femtosecond pulses generated by FWM in Ar [13] and a VUV energy probe QF-16C (Star Tech Instruments), amounted to 45%. The transmission of the single domain SBO, measured with the 160 nm light generated in the RQPM SBO sample (see below) and a photomultiplier tube (PMT 9423, ET-Enterprise), was 63.4%. Refractive indexes of SBO are known from the literature only down to 212.9 nm [8]. To evaluate n_c (essential for the ee-e process) at shorter wavelengths, we measured the spectrum of the SH generated in the a -cut single domain SBO sample (cc-c and bb-c polarization configurations) with a McPherson 0.2 m monochromator Model 234/302 (1200 g/mm grating used in the second and third orders for better resolution), in combination with a VUV-optimized CCD camera Andor D0420-BN-995. The slight wedge (1.8 mrad) made it necessary to reduce the beam diameter to $< 2\text{ mm}$ for proper resolution of the fringes. Measurements were performed for SH at 202 nm (with the frequency-doubled output of the femtosecond Ti:sapphire amplifier) and at 177 and 160 nm

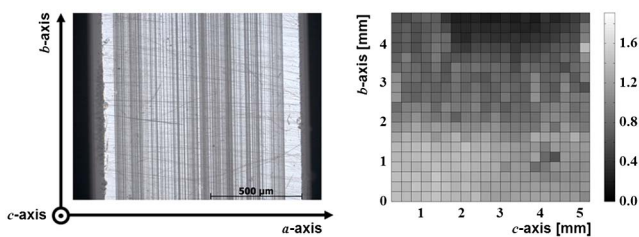


Fig. 1. Photograph of a part of the (001) surface of the SBO sample S7 after etching (left) and transverse mapping for cc-c (ee-e) SHG of femtosecond pulses at 200 nm (right).

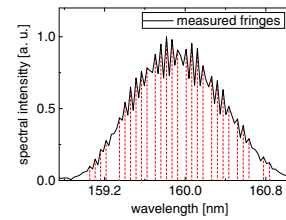


Fig. 2. SH spectrum at 160 nm recorded in the third grating order. The irregular fringe spacing indicates insufficient sampling of the fringes. Nevertheless, the small spacings correspond to 55.7 pm.

(as described below); the spectral resolution was insufficient to resolve fringes at the sixth harmonic $\sim 133\text{ nm}$. The experimental accuracy was evaluated by resolving the SH spectra at 202 nm obtained with three different (cut angle and thickness) type-I β -BaB₂O₄ (BBO) crystals used in non-phase-matched oo-e and ee-e processes: the experimental fringe separation using the second grating order did not deviate by more than 5% from the calculated value.

Figure 2 shows an SH spectrum recorded with the 0.425 mm thick a -cut single domain SBO crystal in cc-c (ee-e) configuration. From such measurements, we estimated the values of $n_c = n_z$ at 202, 177, and 160 nm, and refined the corresponding Sellmeier equation [14].

The experimental setup for tunable VUV SHG of femtosecond pulses is shown in Fig. 3. The fundamental is either the third harmonic (at $\sim 266\text{ nm}$) of the Ti:sapphire regenerative amplifier at 1 kHz or the frequency-doubled output of a commercial optical parametric amplifier (OPA). The third harmonic was generated in a tripling stage (SHG + THG) consisting of two 0.2 mm thick type-I BBO crystals ($\theta = 29^\circ$ and $\theta = 44^\circ$ cuts), a calcite plate (CP) to compensate the group-velocity mismatch, and a half-wave plate (HWP) which rotates the polarization of the $\sim 800\text{ nm}$ wave. The visible output of the OPA (equipped with internal SHG of the signal wave or SFG of signal and pump waves) was additionally frequency doubled in a 0.2 mm thick type-I BBO crystal ($\theta = 44^\circ$ or 65° cut). In both cases, the resulting fundamental UV (242–344 nm) pulse duration was of the order of 70 fs. Depending on the wavelength, the fundamental UV energy varied from 0.2 to 4.7 μJ . These UV pulses were focused onto the RQPM SBO crystal by a curved Al-mirror. The spot size ($1/e^2$ diameter) in the crystal was $\sim 0.44\text{ mm}$.

Figure 4 shows the recorded VUV SH spectra extending down to 121 nm. Good correlation of the position and spectral

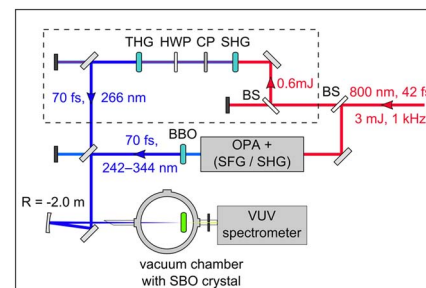


Fig. 3. Experimental setup for tunable SHG in the VUV. BS, beam splitter.

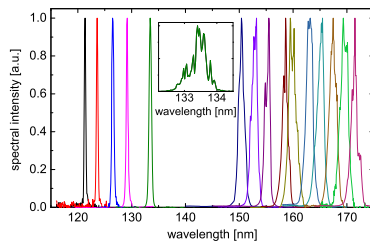


Fig. 4. Spectra of the SH generated in the RQPM SBO sample measured in first order. The inset shows a spectrum at ~ 133 nm measured with higher resolution (third order).

shape was obtained by comparing with the squared spectral intensity of the fundamental; the influence of the random structure on the SH spectra is more pronounced toward longer wavelengths. The spectral features can be seen in the high resolution record of the sixth harmonic shown as an inset in Fig. 4. Fourier transformation yields a lower limit for the expected VUV pulse duration in the absence of chirp; this varies from 35 fs at 172 nm to 105 fs at 121 nm.

The enhancement of the SHG efficiency due to the RQPM crystal structure was evaluated by comparison with the *a*-cut single crystal at an SH wavelength of 160 nm in the cc-c configuration (d_{33}). The fundamental pulses at 320 nm (12 μ J, 70 fs, 1 kHz) were focused by the $R = -2$ m Al mirror onto the SBO crystals in a chamber vacuumated to 10^{-5} mbar. Six dielectric mirrors were used to suppress the fundamental in front of the PMT. To maintain the same voltage of the PMT, four Al-based attenuating filters (Acton Research) were mounted on a motorized stage and introduced into the SH beam only when the RQPM sample was measured. Taking into account the attenuation factor, we obtain an enhancement factor of 9.2×10^4 . Such enhancement is unexpectedly high, much higher than the value of 320 obtained for SH in the 200 nm range with unamplified pulses [11]. It is also much higher than the predictions of a calculation taking into account the resolved domains in this sample (Fig. 1) which, even in the absence of absorption at 160 nm, leads to a factor of ~ 1200 . We attribute this unexpected, but desirable, enhancement to the presence of thin domains that could not be resolved by optical microscopy. Indeed, the calculated coherence length for this process is 375.5 nm, while domains thinner than ~ 500 nm were not well resolved. Note that, for this particular SBO sample (S7), the number of domains was increasing for smaller thickness until the detection limit (Fig. 2e in [15]).

The absolute SHG conversion efficiency was evaluated by generating the sixth harmonic of the Ti:sapphire regenerative amplifier using the cc-c process (d_{33}) in the RQPM SBO sample. By applying six dielectric mirrors that were highly reflective at the sixth harmonic, we were able to separate it and employ a large area AXUV100G (Opto Diode Corp.) photodiode to measure its energy by evaluating the area under the voltage signal recorded by an oscilloscope using a PA-100 amplifier. At the measured wavelength, the diode has an internal quantum efficiency of 1.22 and a response of 0.134 A/W (data sheet of the manufacturer). The input third harmonic was collimated down to a diameter of 1.1 mm by applying two curved mirrors ($R = -0.8$ m and $R = 0.35$ m). The obtained dependence on the input energy is shown in Fig. 5. It can be well fitted

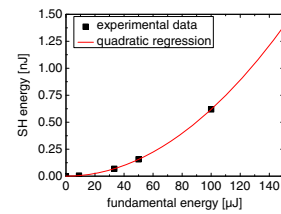


Fig. 5. Dependence of the SHG efficiency for sixth-harmonic generation in the RQPM SBO sample using the cc-c process.

by a quadratic law up to the maximum input level applied, ~ 100 μ J. At this level of fundamental energy, corresponding to an axial fluence of ~ 20 mJ/cm², color centers start to appear in the SBO crystal.

The maximum external SHG efficiency amounts to 6×10^{-6} from Fig. 5. A similar measurement was performed for SH at 160 nm, giving a higher conversion efficiency of 4×10^{-5} . Although the maximum pump fluence was 25% lower in this case (12.3 μ J pulses at 320 nm focused to a diameter of 0.44 mm), the ratio of the SHG efficiencies at 160 and 133 nm is in good agreement with calculations (Fig. 6) that predict a ratio of the order of 8 with the known domain thicknesses for this sample. Figure 6 was computed using the refined Sellmeier coefficients and applying Eq. (4) from [14] to each individual domain. The obtained complex SH spectral electric fields were added up and Fourier transformed. From the obtained temporal intensity profile, the conversion efficiency was finally calculated.

The absolute SHG efficiencies obtained in the present work are higher than the 10^{-5} value reported in [11] for SH at 200 nm using unamplified pulses. However, the experimental conditions, including focusing and pulse duration, are quite different: while the maximum axial pump intensity reached 300 MW/cm² in [11] in the present experiments, we pumped at 225–300 GW/cm². From the absolute SHG efficiency at 160 nm and the relative measurement presented before, one obtains $\sim 5 \times 10^{-10}$ for the efficiency of the non-phase-matched process. In a bb-c SHG process at this wavelength, the efficiency with the RQPM SBO dropped 2.6 times while literature values for the d_{33} and d_{32} coefficients predict a ratio from 1.86 [7] to 3.06 [10].

The occurrence of gray tracks at pump intensities exceeding 300 GW/cm² at 266 nm is not surprising. We observed gray track formation also in the single domain SBO sample when the VUV intensity can be ignored, i.e., the effect is primarily due to the 266 nm fundamental which lies well within the clear transmission range of SBO.

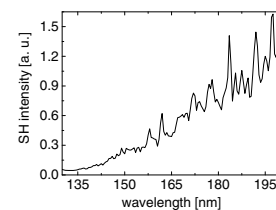


Fig. 6. Numerical simulation of the SHG efficiency dependence on the SH wavelength for the RQPM SBO sample S7, assuming a spectral bandwidth (FWHM) of 6.3×10^{12} Hz for the fundamental.

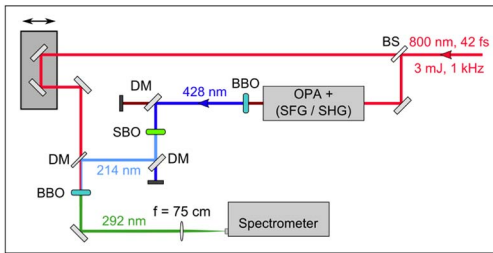


Fig. 7. Experimental setup for pulse duration measurement by DFG. DM, dichroic mirror; BS, beam splitter.

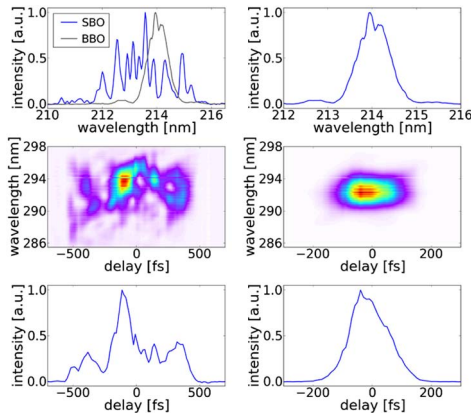


Fig. 8. SH spectra (top), spectrally-resolved cross-correlation (middle) and spectrally integrated intensity of the DFG output near 292 nm (bottom) for SBO (left) and BBO (right).

Temporal characterization of the SH pulses from the RQPM SBO was performed at longer wavelengths in the UV where the energy was higher. However, the main reason for this was the possibility to compare with SHG in BBO, the borate exhibiting the second largest birefringence after the layered KBBF which is not available. To this aim, the output of the Ti:sapphire amplifier was divided into two beams; see Fig. 7. One part was used to pump the OPA and generate 856 nm pulses by internally frequency doubling its idler. These pulses were then again frequency doubled in a 0.3 mm thick type-I BBO cut at 29°. The different colors were separated by dielectric mirrors. The SBO crystal was pumped by the 428 nm beam with $E//b$ for a bb-c (utilizing d_{32} coefficient) process, generating SH light at 214 nm with orthogonal ($E//c$) polarization. This choice was related to the polarization dependence of the available dichroic mirrors characteristics under 45°. The use of type-I interaction permitted direct comparison with a thin (0.1 mm) type-I BBO crystal cut at 65°. In a third 0.1 mm thick BBO crystal (type-I, 55°), the 214 nm pulses at the SH were overlapped with the remaining output of the Ti:sapphire amplifier near 800 nm to produce 292 nm light by difference-frequency generation (DFG). The DFG spectrum was measured at different time delays to record a spectrally resolved cross correlation.

Figure 8 shows the cross-correlation measurements with SH generated in SBO and BBO. As expected, the much thicker SBO sample substantially lengthened the SH temporal shape

due to the group-velocity mismatch. To generate sub-100 fs SH pulses, the sample thickness will have to be reduced to about 0.1 mm. However, a thick sample still offers universal capabilities: it can be used, e.g., for generation of femtosecond pulses at 160 nm by non-degenerate fifth-harmonic generation, i.e., mixing the fundamental and the fourth or the second and the third harmonics. These processes shall exhibit higher conversion efficiency than SHG to 160 nm due to the longer interaction length.

In conclusion, RQPM in SBO is feasible for SHG down to 121 nm and could find applications in generation of coherent radiation deep in the VUV or temporal diagnostics of ultrashort pulses by a reverse second-order nonlinear process. This is the shortest wavelength ever produced with a second-order nonlinear optical process in a solid-state material and, in fact, we have reached the limit set by the available VUV optical materials, such as LiF and MgF₂, used for fabrication of windows, substrates, and refractive optics.

We obtained unexpectedly high enhancement (more than four orders of magnitude, depending on the wavelength), compared with the non-phased-matched case. The obtained SHG conversion efficiency of $\sim 10^{-5}$ starting with an amplified femtosecond Ti:sapphire laser system resulted in single pulse energies on the nJ level at 133 nm (sixth harmonic).

Acknowledgment. The authors thank Svetlana Melnikova and Nikita Radionov (L. V. Kirensky Institute of Physics, Krasnoyarsk, Russia) for the refractive index measurements in the visible.

REFERENCES

1. Y. Nomura, Y. Ito, A. Ozawa, X. Wang, C. Chen, S. Shin, S. Watanabe, and Y. Kobayashi, *Opt. Lett.* **36**, 1758 (2011).
2. C. T. Chen, G. L. Wang, X. Y. Wang, and Z. Y. Xu, *Appl. Phys. B* **97**, 9 (2009).
3. S. Kurimura, M. Harada, K. Muramatsu, M. Ueda, M. Adachi, T. Yamada, and T. Ueno, *Opt. Mater. Express* **1**, 1367 (2011).
4. E. G. Villora, K. Shimamura, K. Sumiya, and H. Ishibashi, *Opt. Express* **17**, 12362 (2009).
5. M. Baudrier-Raybaut, R. Haidar, Ph. Kupecek, Ph. Lemasson, and E. Rosencher, *Nature* **432**, 374 (2004).
6. A. I. Zaitsev, A. S. Aleksandrovsky, A. D. Vasiliev, and A. V. Zamkov, *J. Cryst. Growth* **310**, 1 (2008).
7. V. Petrov, F. Noack, D. Shen, F. Pan, G. Shen, X. Wang, R. Komatsu, and V. Alex, *Opt. Lett.* **29**, 373 (2004).
8. Yu. S. Oseledchik, A. L. Prosvirmin, A. I. Pisarevskiy, V. V. Starshenko, V. V. Osadchuk, S. P. Belokryk, N. V. Svitanko, A. S. Korol, S. A. Krikunov, and A. F. Selevich, *Opt. Mater.* **4**, 669 (1995).
9. F. Pan, G. Shen, R. Wang, X. Wang, and D. Shen, *J. Cryst. Growth* **241**, 108 (2002).
10. A. S. Aleksandrovsky, A. M. Vyunishev, A. I. Zaitsev, A. V. Zamkov, and V. G. Arkhipkin, *J. Opt. A* **9**, S334 (2007).
11. A. S. Aleksandrovsky, A. M. Vyunishev, A. I. Zaitsev, and V. V. Slabko, *Phys. Rev. A* **82**, 055806 (2010).
12. A. S. Aleksandrovsky, A. M. Vyunishev, and A. I. Zaitsev, *Crystals* **2**, 1393 (2012).
13. M. Ghotbi, P. Trabs, M. Beutler, and F. Noack, *Opt. Lett.* **38**, 486 (2013).
14. P. Trabs, F. Noack, A. S. Aleksandrovsky, A. I. Zaitsev, N. V. Radionov, and V. Petrov, *Opt. Express* **23**, 10091 (2015).
15. A. S. Aleksandrovsky, A. M. Vyunishev, A. I. Zaitsev, A. A. Ikonnikov, G. I. Pospelov, V. V. Slabko, and A. A. Zhokhova, *Proc. SPIE* **8071**, 80710K (2011).